




Evaluation of limestone aggregates for railway ballast: particle characteristics and shear strength analysis

Guilherme Faria Souza Mussi de Andrade^{1#} , Cid Almeida Dieguez² ,

Bruno Teixeira Lima¹ , Antonio Carlos Rodrigues Guimarães³ 

Article

Keywords

FIOL
Ballast behavior
Limestone ballast
Heavy-haul railway
Triaxial test

Abstract

The West-East Integration Railway (Ferrovia de Integração Oeste-Leste -FIOL) is an infrastructure project designed to integrate and promote the socio-economic development of the Northeast region of Brazil. In countries with heavy-haul railway operations, there has been increased demand for ballast materials that can withstand cyclic loading of up to 40 tons per axle. In this context, in order to achieve greatest operational efficiency, it is essential to evaluate the characteristics of the limestone aggregate to be used in the ballast layer, as well as the level of cyclic stress that the ballast can withstand. The laboratory investigation consisted of characterization tests, single particle crushing tests, monotonic triaxial tests, and evaluation of the morphological properties of the particles using the Aggregate Image Measurement System. This paper introduces the equipment, describes the experimental procedures, outlines the specimen preparation, and presents the experimental results. The purpose of the study is to estimate the long-term behavior of ballast based on monotonic triaxial tests, the shakedown phenomenon, and the cyclic stress ratio. The results suggest that the cyclic stresses commonly observed in heavy-haul railways may exceed the cyclic stress ratio compatible with the shakedown regime, resulting in a progressive plastic creep regime. Furthermore, the quantity of non-cubic particles exceeds the limits set forth in international ballast standards necessitating a rigorous assessment of the particle shape prior to use in the field.

1. Introduction

The West-East Integration Railway (FIOL, in Portuguese) is a cross-country infrastructure project currently under construction in the states of Bahia and Tocantins, Brazil. With an approximate length of 1,527 kilometers, the railway will connect the municipality of Figueirópolis (junction with the North-South Railway), in the state of Tocantins, to Porto Sul, located in the municipality of Ilhéus, in Bahia. The FIOL project is designed to facilitate integration and socio-economic development between the Northeast, North and Central-West regions of Brazil. The railway will enable the transport of agricultural, mineral, and industrial products via an efficient export route. Due to the importance of this project for Brazil, numerous researchers have studied the behavior of the materials that comprise the infrastructure layers of the FIOL (Santos et al., 2022; Gomes et al., 2023b)

The ballast layer of the FIOL will consist of a limestone aggregate. According to Selig & Waters (1994) and Raymond & Dyaljee (1994), the primary lithologies used in a railway ballast layer include limestone, gneiss, basalt, quartzite,

granite, rhyolite, and dolomite. Recently, recycled materials such as steel slag have been the subject of extensive research as an alternative to crushed rock aggregates for use in ballast layers (Delgado et al., 2019; Esmacili et al., 2019; Esmacili et al., 2020; Chamling et al., 2020; Jing et al., 2020; Guimarães et al., 2021; Indraratna et al., 2022; Gomes et al., 2023a). Despite this, the technical standards established by international institutions to guide the use of materials in the ballast layer prohibit the use of limestone (sedimentary rock) and alternative materials (REFER, 2015). The most recent Brazilian standard for railway ballast (ABNT, 2021) permits the use of various types of limestone and other lithologies. However, there is considerable concern regarding the efficiency of the limestone ballast to be used in the FIOL project.

The use of crushed rock in the ballast layer is one of the most demanding applications for these materials (Paixão et al., 2016). The stresses imposed by the passage of trains present the greatest challenge to the understanding and application of the materials that make up the ballast layer. Railway deterioration is primarily attributable to the permanent deformation of the ballast layer resulting from the

#Corresponding author. E-mail address: guimussi@hotmail.com

¹ Universidade do Estado do Rio de Janeiro, Rio de Janeiro, RJ, Brasil

² Universidade Federal do Rio de Janeiro, COPPE, Rio de Janeiro, RJ, Brasil

³ Instituto Militar de Engenharia, Rio de Janeiro, RJ, Brasil

Submitted on November 20, 2023; Final Acceptance on June 27, 2024; Discussion open until February 28, 2025.

<https://doi.org/10.28927/SR.2024.011223>



This is an Open Access article distributed under the terms of the Creative Commons Attribution License, which permits unrestricted use, distribution, and reproduction in any medium, provided the original work is properly cited.

passage of trains and track maintenance operations (Guo et al., 2018). A precise understanding of this matter helps to prevent accelerated deterioration and premature failures that can lead to interruptions in railway operations (Indraratna & Ngo, 2018). According to Delgado et al. (2022), there has been a noticeable increase in demand for ballast materials that can withstand cyclic loading of up to 40 tons per axle. This is mainly due to the growing interest in trains with heavier axle loads and longer train compositions, particularly in countries with heavy-haul railway operations. In order to achieve greatest efficiency in the FIOIL rail operations, it is necessary to assess the level of cyclical stresses that the limestone ballast can withstand. Laboratory methods that can predict the shear strength of the crushed rock aggregate provide a valuable resource for evaluating ballast effectiveness and enabling more cost-effective designs.

The plastic behavior of ballast is influenced by the cyclic stress ratio (n) as defined in Equation 1 (Suiker, 2002). Suiker et al. (2005) found that for low values of the cyclic stress ratio, $n < 0.82$, the rate of permanent deformation at 1,000,000 load cycles becomes negligible. In other words, the cyclic response of the ballast becomes almost elastic, a phenomenon known as “shakedown” (Werkmeister et al., 2001). Therefore, it is essential to determine the shear strength of the ballast in order to characterize the level of cyclic stress to be used in repeated loading tests. This allows for the prediction of whether the response of the material will remain in the shakedown regime.

$$n = \frac{q_{cyc}}{q_f} \quad (1)$$

where: q_{cyc} is the range of cyclic deviatoric stress to be applied in the repeated load triaxial tests and q_f is the deviatoric stress at failure obtained from the monotonic triaxial tests under the same stress path.

A comprehensive understanding of the mechanical behavior, physical properties, and individual characteristics of the particles, including the crushing strength of the grain and the morphological characteristics of the aggregate to be used in the ballast layer, is essential for the successful implementation of this project. Laboratory research was conducted to verify that the material meets the specifications of the Brazilian standard for railway ballast (ABNT, 2021). Moreover, an estimate of strength and characterization of the level of cyclic stress to be imposed by the passage of trains is carried out to ensure that the resulting permanent deformation rate is negligibly small. This research represents a novel approach to estimating the behavior response of limestone ballast from monotonic triaxial tests. The methodology draws upon the shakedown phenomenon (Werkmeister et al., 2001), the stresses frequently observed in heavy-haul railways (Delgado et al., 2021) and the cyclic stress ratio (n) concept proposed by Suiker et al. (2005).

The present study involved a comprehensive laboratory investigation with the objective of evaluating the efficiency of limestone aggregate for use in the ballast layer of the FIOIL. The mandatory tests specified in NBR 5564 (ABNT, 2021) were performed, in addition to some optional tests. In addition, the individual characteristics of the particles, including tensile strength and morphological properties (Figure 1), were analyzed using grain crushing tests and an advanced digital image processing technique, respectively. Finally, the shear strength of the material was evaluated using monotonic triaxial tests. The results were used to determine whether the cyclic stresses frequently observed in heavy-haul railways (Delgado et al., 2021) meet the cyclic stress ratio limit for the material to remain in the shakedown regime (Suiker et al., 2005). Finally, the conclusions drawn from the experimental approach are presented, along with a discussion of its limitations.

2. Materials and methods

2.1 Material description

The ballast used in the laboratory investigation is composed of crushed limestone particles. Ballast is produced by crushing rock and sieving it to obtain the desired particle sizes. The grain-size distribution of the ballast material is depicted in Figure 2. The ballast meets the gradation specified in AREMA No. 4 in the Manual for Railway Engineering (AREMA, 2020). The ballast is classified as poorly graded gravel, in accordance with the definitions of the *Unified Soil Classification System* (USCS) and the Brazilian standard NBR 6502 (ABNT, 1995), as evidenced by the values of the coefficient of uniformity (C_u) and the coefficient of curvature (C_c) of the particle size distribution PSD curve, which were

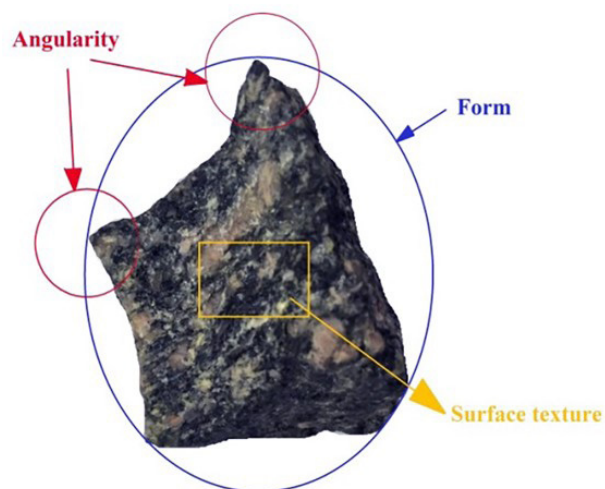


Figure 1. Shape characteristics of ballast particle (reproduced from Guo et al., 2018)

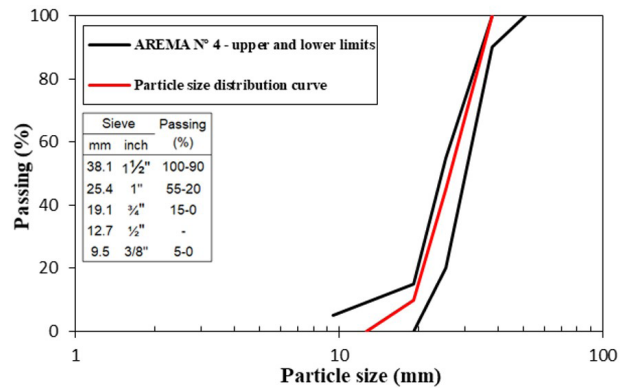


Figure 2. PSD curve of limestone ballast.

1.61 and 0.98, respectively. The primary rationale for using the AREMA N° 4 ballast standard was its use in main railway lines, thus allowing triaxial tests to be conducted without using the parallel gradation technique. This is because the use of scaling-down techniques still has limited acceptance among several authors (Indraratna et al., 1998; Klinecivius, 2011).

A series of characterization tests were conducted to ascertain the physical properties of the ballast, including particle shape, the number of non-cubic particles, apparent specific mass, apparent porosity, water absorption, weather resistance, the unit mass limit in the loose state, powdery material, clay lumps, the Los Angeles abrasion index and Treton shock resistance index. All tests were conducted in accordance with the recommendations of the Brazilian standard (ABNT, 2021), which establishes specifications and test methods for railway ballast. The results were compared with the limits established by both the Brazilian standard and the AREMA Railway Engineering Manual (AREMA, 2020). Only the quantity of non-cubic particles exceeded the limit allowed by both ballast specifications, as shown in Table 1.

2.2 Specimen preparation

The preparation of the ballast specimen involved the placement and compaction of four layers of equal thickness via vibration within a tripartite mold. Initially, a latex membrane of 2.0 mm thickness was manually placed against the wall of the compaction mold. The thickness of the latex membrane was necessary to prevent puncturing of the membrane by the sharp edges of the ballast particles. The specimen compaction process involved the application of vibration to each layer for a period of one minute, followed by a fifth vibration cycle of two minutes, using a vibrating plate. Once the compaction process was complete, the test specimen was adjusted manually to ensure that the particles were optimally positioned at the top of the specimen.

To regularize the top surface of the specimens, a layer of gypsum plaster was applied, and the surface was smoothed with the use of a glass plate coated with petroleum jelly.



Figure 3. Specimen prepared for monotonic triaxial tests.

Finally, to correct the parameters of the PSD, the excess material was sieved and weighed, with the resulting mass subtracted from the initial mass. After 24 hours, the specimen was placed in the triaxial apparatus. Subsequently, the top cap was attached, and the tripartite mold was removed while maintaining a temporary internal vacuum to support the specimen (Figure 3). A similar procedure for preparing the specimens was carried out by Silva (2018), Rosa et al. (2021), Cescon (2021), and Gomes et al. (2023a).

Specimens prepared following the same experimental procedure exhibited consistent void ratios. The void ratio of the ballast specimens was found to be 0.83, 0.79 and 0.82. The process of compacting the test specimen was considered to be effective, as the resulting values for the initial void ratio (e_0), coefficient of uniformity, and coefficient of curvature were comparable to those reported by Indraratna & Salim (2003), Indraratna et al. (2007) and Anderson & Fair (2008) for ballast materials with uniform particle size distributions.

The tripartite mold used to prepare the ballast specimens has a nominal height of $H = 300$ mm and a nominal diameter of $D = 150$ mm, yielding an aspect ratio of $H/D = 2.00$, a recommended ratio to minimize the effects of friction at the ends of the sample (Bishop & Green, 1965). The maximum particle diameter (d_{max}) in the uniformly graded ballast material

Table 1. Ballast properties in comparison with international standard limits.

Property	Studied Limestone	NBR 5564 (ABNT, 2021)	AREMA (2020)
Average particle shape	Cubic	Cubic	Cubic
Non-cubic particles (%)	18	< 15	< 5
Apparent specific mass (kg/m ³)	2,703	> 2,600	> 2,600
Apparent porosity (%)	0.17	< 2	-
Water absorption (%)	0.06	< 2	< 2
Powdery material (%)	0	< 1	-
Clay lumps (%)	0	< 0.5	< 0.5
Unit mass limit in the loose state (kg/m ³)	1,385	> 1,250	-
Los Angeles abrasion index (%)	22	< 30	< 30
Treton shock resistance index (%)	12.3	< 25	-
Weather resistance (%)	4.75 (63.5 to 38 mm) 1.90 (38 to 19 mm) 3.47 (19 to 12.5 mm)	< 10	< 5

is 25 mm, as illustrated in Figure 3. This corresponds to a ratio between the specimen diameter and the maximum particle diameter of $D/d_{max} = 6$. Skoglund et al. (2000) recommended that a representative sample size should have a D/d_{max} ratio in the range of 5-7, and Indraratna et al. (1993) proposed a value of 6 at which the scale effects become negligible.

2.3 Experimental setup of monotonic triaxial tests

The shear strength of ballast under monotonic loading was investigated using a large-scale triaxial apparatus. Constant confining air pressure was applied to the acrylic chamber through an air compressor. A series of three isotropically consolidated drained triaxial tests (CID) were conducted, with constant confining pressures (σ'_c) of 40, 55 and 70 kPa. The confining pressures employed were maintained within the realistic range of 10-70 kPa, following the recommendations of Indraratna et al. (2013a). The strain rate used in the monotonic triaxial tests was 0.83 mm/min, which is consistent with the strain rates employed by Anderson & Fair (2008) and Aursudkij et al. (2009) in their respective tests.

In this type of test, failure is not easily defined due to the constant fluctuation in the deviator stress resulting from the “stick-slip” processes between individual ballast particles. In other words, the ballast particles that are in contact slide over each other, resulting in an irregular movement, characterized by brief accelerations with interruptions. These local instabilities are observed at the level of the specimen due to the large ratio between the average size of the ballast particles and the size of the specimen. Similar behavior was reported by Suiker et al. (2005), Anderson & Fair (2008), and Chamling et al. (2020).

The instrumentation consisted of a potentiometric displacement transducer installed on the top of the triaxial cell, a 2-ton load cell, a pressure gauge, a data acquisition system, and a notebook computer. Pressure regulation was provided through an external pressure control system.

The potentiometric transducer allowed displacements of up to 100 mm, which proved sufficient for the large deformations required. The experimental data was collected automatically every second, ensuring precise stress-strain curve definition during the tests. Unfortunately, it was not possible to measure the volumetric change during the tests, since the specimens were not saturated, and no instrumentation was used to measure the radial displacements.

All vertical and lateral stress measurements were corrected for the membrane effect in accordance with the methodology outlined in the standard procedure ISO 17892-9 (ISO, 2018).

2.4 Particle morphology analysis

Particle morphology has a direct impact on the performance and deformation of granular material layers, such as railway ballast (Saint-Cyr et al., 2009). However, the traditional methods employed for particle morphology evaluation are inadequate, resulting in inconclusive test results and controversial conclusions (Tafesse et al., 2012; Ionescu, 2004). Consequently, advanced digital image processing techniques have been developed (Tutumler et al., 2009; Greer & Heitzman, 2017). These methods are more efficient than traditional methods and provide more accurate particle morphology evaluation and corresponding morphological properties, such as particle size distribution, volume, surface area, form (flat or elongated ratio, sphericity), angularity index and surface texture index (Mvelase et al., 2012). The advantages and disadvantages of different apparatuses used to assess morphological properties are presented by Guo et al. (2019).

In this study, the Aggregate Image Measurement System (AIMS) was used (Figure 4). The AIMS provides a means of quantifying morphological properties, including sphericity, angularity, and surface texture of the particles, through digital evaluation of a set of particles using bidirectional images correlated with the field of view depth (Al-Rousan, 2004).



Figure 4. Aggregate Image Measurement System (AIMS).

The apparatus is composed of one camera and two distinct types of illumination for capturing images with varying resolutions. The particles are initially deposited in a compartment of a rotating circular lighting table. The image capture software then carries out three asynchronous measurement cycles on the perimeter of the particles (Delgado et al. 2022).

AIMS quantifies sphericity through the three dimensions of the particle under analysis. According to Fletcher et al. (2003), the camera and microscope assembly provide projections of the particles, which are used to measure the longest, shortest, and intermediate dimensions of each particle. The Sphericity Index (*SP*) value varies within the range of 0–1, where an *SP* of 1 indicates that a particle has equal dimensions. Angularity is defined as the measure of the presence of sharp corners in particles (Masad, 2003). The AIMS software quantifies angularity through the gradient technique, whereby a higher gradient value indicates a higher angularity. The software estimates the changes in the inclination of the gradient vectors and returns an average Angularity Index (*AI*) value, ranging from 0 to 10,000, where a perfectly rounded particle has an *AI* of 0. Surface texture is defined as the irregularity of the particle surface on a very small scale that is not affected by the general grain shape (Al-Rousan, 2004). The AIMS software quantifies the particle surface texture through the wavelet method, which employs three separate images to provide details of the texture in the horizontal, vertical, and diagonal directions. The Texture Index (*TI*) value varies within the range 0–1,000, with *TI* equal to 0 corresponding to a completely smooth particle surface. Further details on the methods and techniques used by AIMS to determine

the morphological properties of particles can be found in Fletcher et al. (2003), Al-Rousan (2004), and Delgado et al. (2022).

The AIMS was compared against other test methods that measure aggregate morphology properties and the results were found to be satisfactory. The comparison was conducted based on statistical analysis in terms of accuracy, repeatability, reproducibility, costs, and operational characteristics (ease of use and interpretation of results). The analysis incorporated aggregates from different geographic locations, rock types and shape characteristics (Al-Rousan, 2004). In recent years, the AIMS has been employed by numerous Brazilian researchers engaged in the investigation of the morphological properties of their respective railway ballast (Rosa et al., 2021; Cescon et al., 2021; Delgado et al., 2022).

The morphological properties of the limestone aggregate were quantified through three sets of 50 particles with different nominal diameters (12.7, 19.0 and 25.4 mm) that comprise the PSD curve of the specimens. The criteria used to define the ranges for morphological properties classification were derived from the Ibiapina et al. (2018) proposal, as it is a classification system developed with aggregates obtained from various regions of Brazil.

2.5 Fracture strength of ballast grains

It is well established that particle fracture (tensile strength) plays a significant role in the behavior of crushable aggregates (McDowell & Bolton, 1998). The tensile strength of rock grains can be indirectly measured by diametral compression between two flat plates (Jaeger, 1967), as

illustrated in Figure 5a. In their respective works, Lee (1992) and McDowell & Bolton (1998) describe the characteristic particle tensile strength (σ_f) as follows:

$$\sigma_f = \frac{F_f}{d^2} \quad (2)$$

where: F_f is the maximum load corresponding to the fracture of the particle and d is the initial particle diameter.

In their 2001 study, Festag & Katzenbach distinguished between two primary mechanisms underlying grain crushing: grain fracture and grain abrasion. Grain fracture, which occurs under conditions of high stress, involves the separation of grains into parts of nearly the same size. In contrast, grain abrasion is an independent process that occurs at any stress level, resulting in detachment of very small particles from the grain surface. When the stress level is low in comparison to the particle strength, grain fracture may be limited. However, grain abrasion persists as a continuous phenomenon (Festag & Katzenbach, 2001).

As stated by Indraratna & Salim (2003), ballast degradation is a complex phenomenon influenced by multiple factors, including amplitude, frequency, number of load cycles, aggregate density, angularity of particles, confining pressure, and degree of saturation. However, the authors emphasize that the fracture resistance of the particles is the most significant factor that controls the breakage of ballast. The tensile strength of the particles has a direct inverse relationship with the degradation of the ballast.

The single particle fracture strength of limestone ballast was measured in the laboratory to evaluate the relationship between tensile strength and particle diameter under comparable loading and boundary conditions. For these tests, a uniaxial loading frame was used, with a strain rate of 1.27 mm/min. Since the ballast met the gradation specification of the AREMA standard No. 4, thirty-five particles with a diameter of 10-50 mm were selected for testing. Each particle was positioned between the top and bottom plates of the compression machine, allowing for the initial particle diameter to be determined

prior to the start of the test (Figure 5b). The maximum load corresponding to the fracture of the particle was recorded, and the tensile strength was estimated using Equation 2, which is consistent with the definition of tensile strength of concrete in the Brazilian test.

A larger number of tests were conducted, but many were subsequently excluded due to the following issues: i) particle breakage along a preferential plane due to the presence of discontinuities; ii) the breaking of grain edges which did not represent crushing rupture.

3. Results and discussion

3.1 Morphology of limestone particles

A qualitative analysis of the morphological properties was initially performed using three surface microscopy images and three 2D images of angularity obtained from the AIMS (Figure 6a and 6b, respectively). The images shown are of particles randomly selected from those analyzed. In terms of surface texture, the microscopic images appear to show different characteristics. Larger diameter particles appear visually smoother than smaller diameter particles. However, in terms of angularity, the different particle diameters do not appear to exhibit distinct characteristics.

After qualitative analysis of the images, the initial assumptions were validated by measuring the morphological properties of the limestone aggregate using the AIMS software. The results of the sphericity, angularity, and texture of the three sets of 50 particles from each of the nominal diameters that comprise the PSD curve of the specimens are shown in Figure 7.

Figure 7a illustrates the relationship between particle diameter and sphericity. It demonstrates that as particle diameter decreases, sphericity also decreases. This finding is consistent with that of Rosa (2019). However, despite this finding, the majority of the particles were classified as having low sphericity, with only a small number of particles

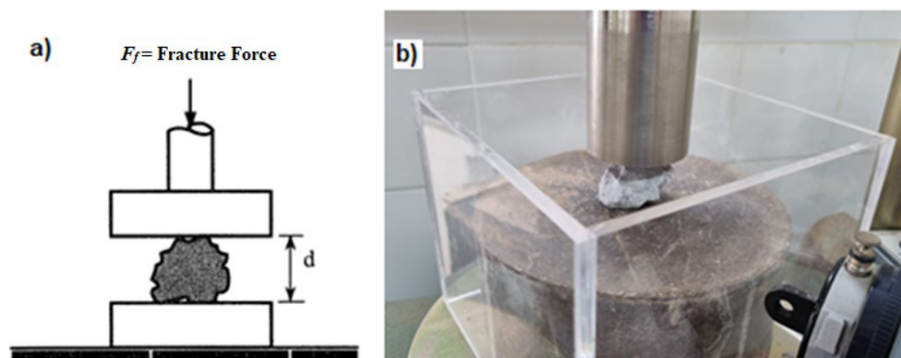


Figure 5. Single particle fracture strength test. (a) Test set-up (Indraratna & Salim, 2003); (b) Limestone ballast particle under test.

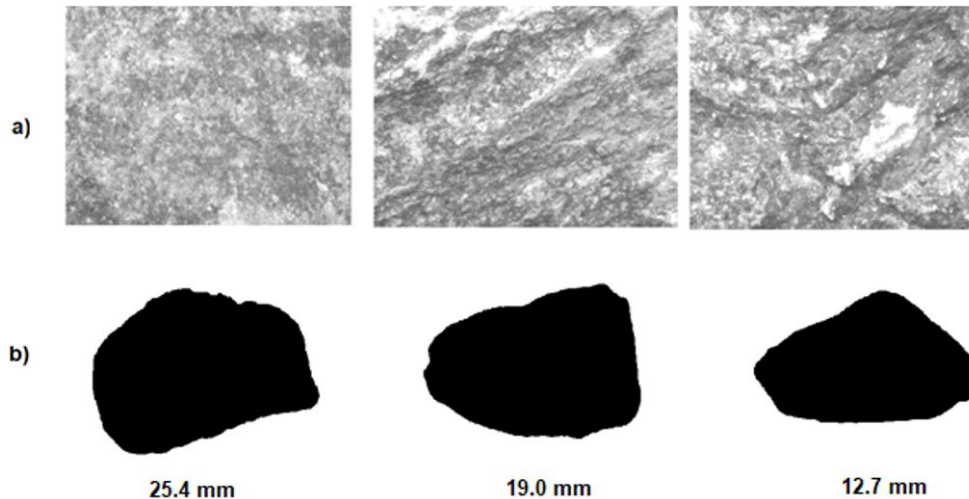


Figure 6. (a) AIMS surface microscopy images; (b) AIMS 2D images.

in the moderate sphericity range. Approximately 30% of the particles with a diameter of 12.7 mm were classified as flattened/stretched.

As noted in Al-Rousan (2004), sphericity values provide an effective indication of the proportions of a particle's dimensions. However, sphericity is insufficient for assessing the lamellarity of particles. Therefore, the F&E correlation, shown in a Zingg (1935) diagram, is necessary. In this correlation, the flatness ratio (F) is calculated as the ratio of the particle's shortest dimension (S) to its intermediate dimension (I), while the elongation ratio (E) is determined as the ratio of the intermediate dimension to the largest dimension (L). The Zingg diagram provides a comprehensive understanding of the lamellarity level of the particles and can serve as a valuable tool for establishing limits on the morphological characteristics of ballast particles (Delgado et al. 2022).

The F&E correlation for the limestone ballast is shown in Figure 8, along with the maximum acceptable F&E limits for ballast particles indicated in the Brazilian standard (ABNT, 2021) and the American standard (AREMA, 2020). Although the limit required by the Brazilian standard is more restrictive (1:2) compared to that indicated by the American standard (1:3), a wider tolerance range is allowed in Brazil (15%) than in the USA (5%), as shown in Table 1.

As illustrated in Figure 8 the majority of the particles analyzed in the AIMS exhibited a markedly variable shape, with a considerable dispersion of values in the Zingg diagram. A significant number of points fell below the recommended normative limits. The shape of the particles is not suitable for use as ballast material, as non-cubic particles tend to align themselves in a preferential direction (vertically or horizontally), forming planes of weakness, as well as being subject to greater wear due to abrasion and particle breakage.

The angularity of the particles was observed to be nearly identical, with the curves practically overlapping

(Figure 7b). This indicates that the angularity of the limestone ballast is not influenced by the different particle diameters, confirming the assumptions made in the qualitative analysis of the 2D images (Figure 6b). The angularity of the particles can be classified as subrounded in almost all cases, with a few particles in the subangular range.

Among the morphological properties measured, it is evident that the surface texture was most significantly influenced by the variation in diameters analyzed. There is a discernible tendency for the surface texture to increase as the particle diameter decreases (Figure 7c). As with the angularity of the particles, the Texture Index measurement conducted by AIMS corroborated the assumptions made through the surface microscopy images (Figure 6a). The majority of the particles analyzed were classified as low or moderate texture.

3.2 Tensile strength of ballast grains

Grain crushing is promoted by angularity, coarseness, uniformity of gradation, low particle strength, stress level and anisotropy. However, according to Indraratna & Salim (2003), the grain resistance to fracture is the most important factor. Figure 9 shows the tensile strength of thirty-five limestone ballast particles, with a diameter of 10-50 mm. There is considerable dispersion in the tensile strength results. It is important to note that tensile strength decreases with increasing grain size. This trend has been similarly documented by McDowell & Bolton (1998), Nakata et al. (2001), Indraratna & Salim (2003) and Delgado et al. (2021), for a variety of materials. This phenomenon can be attributed to the fact that larger particles tend to contain a higher number of flaws or defects, thereby increasing the probability of a defect being present in the particle that will break (Lade et al., 1996).

The lower tensile strength obtained in the particle crushing tests suggests that the larger diameter particles

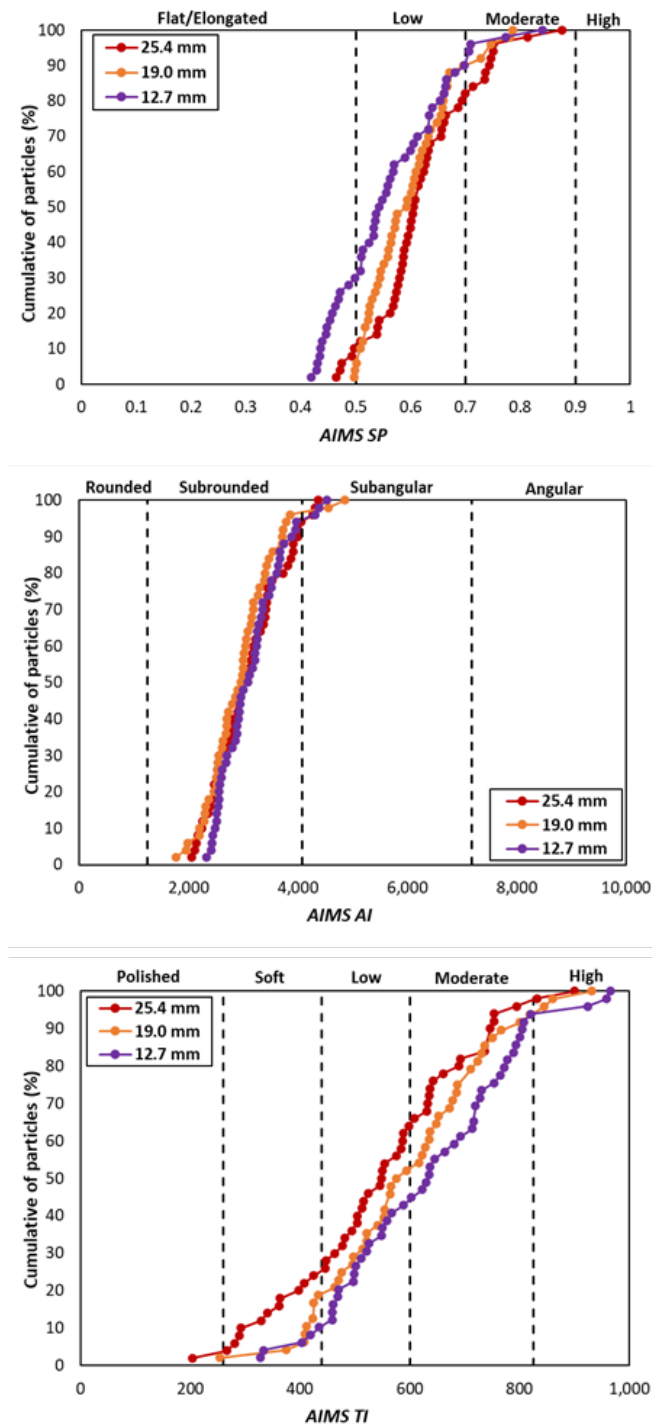


Figure 7. AIMS particle morphology measurement: (a) Sphericity; (b) Angularity; (c) Surface texture.

are subject to more pronounced grain breakage. This can be quantified after the long-term permanent deformation tests. However, this premise cannot be evaluated due to the impossibility of conducting repeated load triaxial tests, which is a limitation of the current study.

3.3 Monotonic triaxial tests

A series of three isotropically consolidated drained triaxial tests were conducted with constant confining pressures of 40, 55, and 70 kPa. Based on the test results, the shear strength

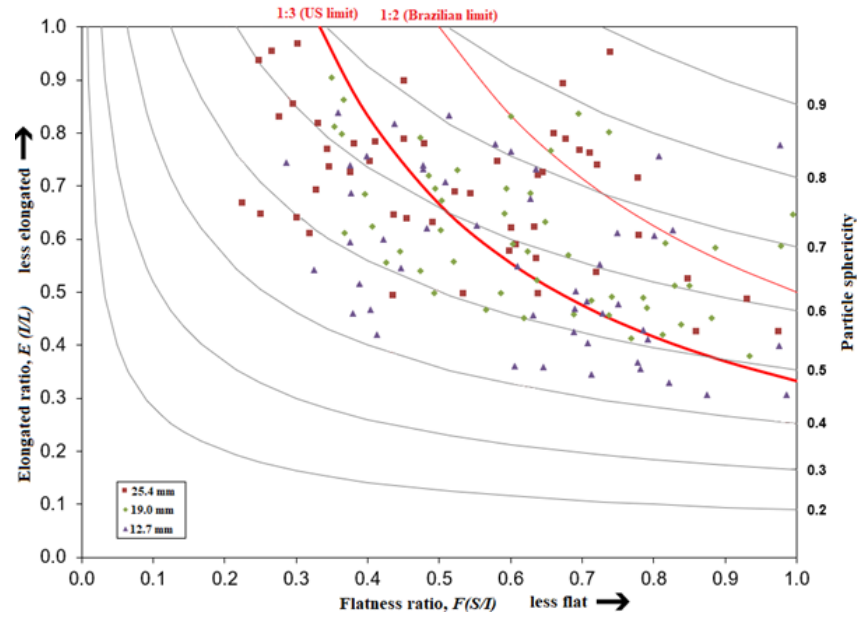


Figure 8. $F&E$ correlation for limestone ballast particles presented in a Zingg diagram.

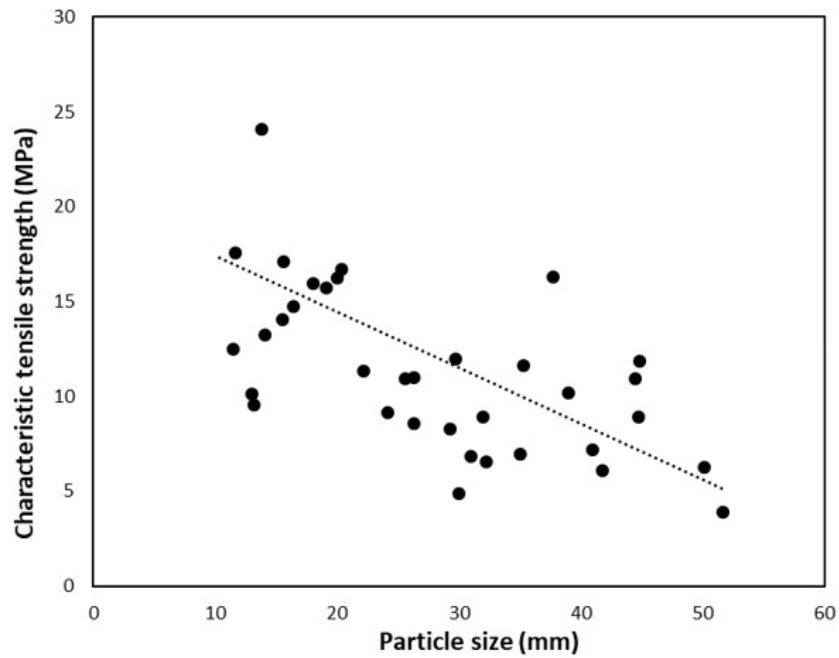


Figure 9. Single particle crushing strength test results.

parameters of the limestone aggregate were determined, and the shear strength of the ballast was compared with the stresses frequently observed on heavy-haul railways. Consequently, the resulting cyclic stress ratios were evaluated to ascertain whether they fell within the limit value of 0.82, as proposed by Suiker et al. (2005), to ensure that the ballast remained in shakedown regime. As stated by Delgado et al. (2022),

the cyclic deviatoric stress (q_{cyc}) values of 280 and 350 kPa are representative of heavy-haul freight trains with 32.5 and 40 t/axle, respectively.

The shape of the grains affects contact tensions. Due to the typical particle size of ballast, grain-to-grain contact is very intense, as there is no matrix of fines to reduce these contacts. The high concentration of non-cubic particles in

the analyzed limestone ballast suggests that the shape of the grain may influence the macroscale behavior. However, this effect has not been fully modeled and will be verified in future research.

The stress-strain curves, measured at each confining pressure, have been plotted in Figure 10a. Initially, it was found that the behavior of the ballast during shear was non-linear. As the confining pressures increased, the deviatoric stress also increased. Additionally, ballast softening was absent during shear, which is attributed to the loose arrangement of ballast particles due to the uniform character of the particle size distribution adopted (AREMA N. 4, see Figure 1). A comparable result was reported by Suiker et al. (2005), who also conducted tests with a PSD curve that met the specifications of AREMA N. 4.

The observed lack of smoothness in the curves may be attributed to the occurrence of “stick-slip” during shearing, breakage of the ballast, or a combination of both. Anderson & Fair (2008) also reported this phenomenon when they conducted monotonic triaxial tests on granite ballast of uniform granulometry with confining pressures varying between 40 kPa and 140 kPa. Chamling et al. (2020) observed the same phenomenon in tests with steel slag ballast specimens

and granite ballast with confining stresses varying between 40 kPa and 80 kPa.

Despite the stress-strain curves exhibiting a lack of smoothness, stabilization of the deviatoric stress was considered for large deformations ($\geq 17\%$), when it was close to a horizontal trend. This stabilization was considered indicative of the material having reached the critical state, given that it was not possible to measure the volume change of the specimens during shearing.

Figure 10b depicts the Effective Stress Path (ESP) and the Critical State Line (CSL) for the three tests, plotted in the $p'-q$ plane. Table 2 provides a summary of the monotonic triaxial test results. The friction angle at the critical state (φ'_{cv}), which is an intrinsic parameter of soils and granular materials, and the critical state friction coefficients (M), which were obtained for limestone aggregate, were 50.7° and 2.08, respectively. Aursudkij et al. (2009) also conducted monotonic triaxial tests with limestone ballast, using PSD curves characteristic of uniformly graded granular materials, a similar D/d_{max} ratio, comparable bulk density (Table 2) and similar strain rate. The results presented by those authors align with those obtained in the present research, particularly when the confining stresses were equivalent.

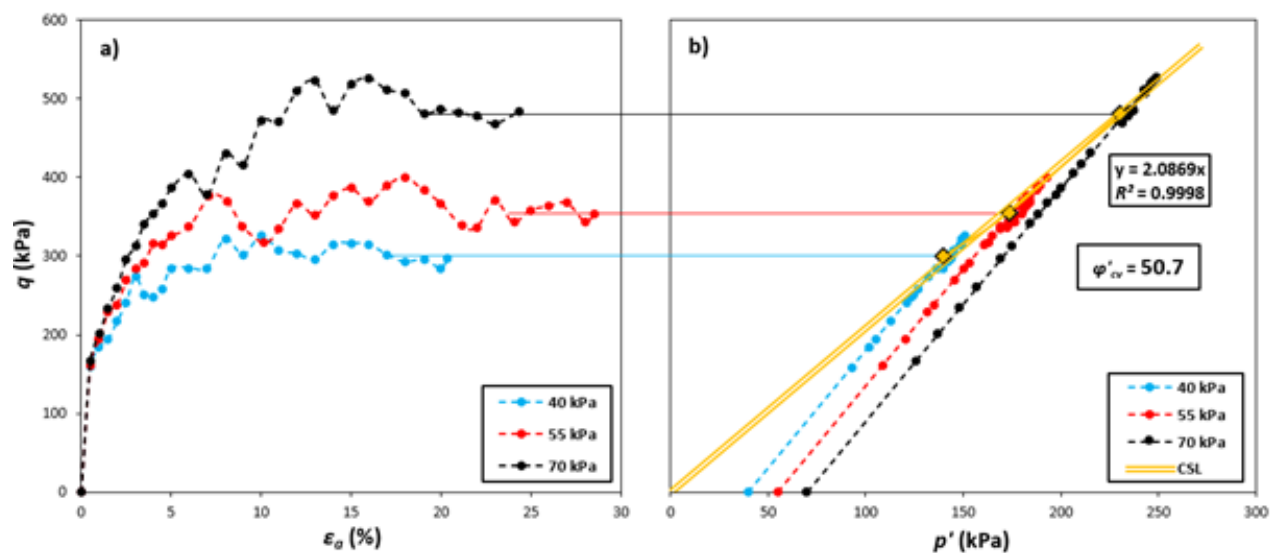


Figure 10. Monotonic triaxial test results of limestone aggregate: (a) stress-strain curves; (b) CSL envelope.

Table 2. Experimental characteristics and monotonic triaxial tests results.

Test	σ'_3 (kPa)	Density (kg/m ³)	e_0	q_f (kPa)	M	Φ'_{cv} (°)
MT 1	40	1,475	0.83	300		
MT 2	55	1,507	0.79	355	2.08	50.7
MT 3	70	1,486	0.82	481		

Note: MT = Monotonic triaxial; $M = p'/q$ = Critical state friction coefficient; p'' = mean effective stress; q = deviatoric stress.

Table 3. Cyclic stress ratio estimated using representative cyclic deviator stress of heavy-haul freight trains with 32.5 and 40 t/axle.

σ'_3 (kPa)	q_f (kPa)	q_{cyc} (kPa)*	n
40	300	280	0.93
55	355	280	0.79
70	481	280	0.58
40	300	350	1.17
55	355	350	0.99
70	481	350	0.73

* According to Delgado et al. (2022).

The cyclic stress ratio (n) was estimated using Equation 1, based on the deviator stress at break obtained in the monotonic triaxial tests and the cyclic deviator stresses representing heavy-haul freight trains with 32.5 and 40 t/axle, as proposed by Delgado et al. (2022). The results are shown in Table 3. As can be seen, for the cyclic deviatoric stress representing the 32.5 t/axle train, both the cyclic stress ratio for the test with 55 and 70 kPa of confining pressure yielded values below the limit of 0.82 proposed by Suiker et al. (2005). In other words, in these two cases, the permanent deformation rates are expected to be extremely small and therefore the material would be in shakedown regime. However, the same behavior was not obtained when considering the cyclic deviatoric stress representing the 40 t/axle train. The cyclic response of the ballast would be considered almost elastic only for the cyclic stress ratio of the test with 70 kPa of confining pressure. This phenomenon illustrates the significance of methodologies designed to increase the horizontal stresses that confine the ballast and, consequently, increase the stability of the track. Such methodologies include the use of geogrids (Indraratna et al., 2013b).

The results indicate that extreme caution should be exercised when the cyclic stress ratio exceeds the 0.82 limit, given that long-term behavior under cyclic loading can lead to a progressive plastic creep regime (Werkmeister et al., 2001). However, the long-term behavior of limestone ballast remains unproven due to the unavailability of repeated load triaxial tests.

4. Conclusion

Laboratory experiments were conducted to evaluate the efficiency of the limestone aggregate for use in the ballast layer of FIOL. The physical properties, tensile strength, morphological properties, and shear strength of the ballast were evaluated. In these experiments, all specimens were prepared in the same way, and the results demonstrated that the methodology used was effective. The specimens were classified as poorly graded gravel, and the PSD curve complied with the specifications of AREMA No. 4. The initial void ratio, coefficient of uniformity, and coefficient of curvature were comparable to those observed in previous studies using

different compaction procedures (Indraratna & Salim, 2003; Indraratna et al., 2007; Anderson & Fair, 2008).

Among the physical properties of the ballast, it was determined that the quantity of non-cubic particles exceeded the established limits set forth by the international standards analyzed. With regard to the morphological properties, the surface texture was found to be most influenced by the variation in diameters analyzed, with smaller particles exhibiting a higher Texture Index. Additionally, it was noted that smaller particles exhibited greater tensile strength. The findings suggested that smaller particles tend to show a reduced incidence of grain breakage after long-term permanent deformation tests.

The monotonic triaxial tests were conducted up to large deformations, allowing for the determination of the shear strength parameters and the critical state line. The cyclic stress ratio (n) was identified as a critical parameter in predicting ballast behavior. Therefore, the increase in axle loads of trains traveling on railways is a phenomenon that must be carefully assessed. The results suggest that the shakedown phenomenon, which is characterized by an almost elastic behavior, occurred in the case representing the 32.5 t/axle train, when the confining pressures were 55 kPa and 70 kPa. Conversely, for the 40 t/axle train, the shakedown regime was reached only at the highest levels of confining pressure.

The first limitation of the research was the impossibility of measuring the volume change of the specimen during the monotonic triaxial tests. Consequently, it was not possible to determine whether the behavior of the ballast was dilatant or contractile during shear. In this research, it was not possible to carry out repeated load triaxial tests to assess the long-term behavior of the limestone ballast and, consequently, the grain size breakage. This represents the main limitation of the present experimental investigation. To achieve greater accuracy, it would be advisable to conduct repeated load triaxial tests with the deviatoric cyclic stress proposed by Delgado et al. (2022) and evaluate the rate of permanent deformation at 1,000,000 load cycles. Furthermore, a logical next step would be to sieve the specimens, following the completion of the tests in order to quantify the extent of grain breakage in terms of the index of particle breakage, B_g (Marsal, 1965) and the ballast breakage index, BBI (Indraratna et al., 2005).

The experimental research yielded crucial insights regarding the efficiency of the limestone ballast under study, as well as providing prediction of the behavior of this material in the face of the cyclic stress frequently observed in railways. To ensure the durability and efficiency of the railway ballast material, it is crucial that the particle shape specifications are met. Nevertheless, further laboratory tests, such as the repeated load triaxial test, are necessary to validate the assumptions made in this study.

Acknowledgements

The authors would like to thank the COPPE for making their laboratory available for this project. This study was financed

in part by the Coordenação de Aperfeiçoamento de Pessoal de Nível Superior – Brasil (CAPES) – Finance Code 001.

Declaration of interest

The authors have no competing interests to declare. All co-authors have reviewed and approved the content of the paper and have no financial interests to declare.

Authors' contributions

Guilherme Faria Souza Mussi de Andrade: conceptualization, formal analysis, investigation, methodology, data curation, validation, visualization, writing – original draft. Cid Almeida Dieguez: investigation, data curation. Bruno Teixeira Lima: supervision, validation, resources – review & editing. Antonio Carlos Rodrigues Guimarães: supervision, validation, resources – review & editing.

Data availability

The data sets generated and analyzed in the course of the current study are available on request from the corresponding author.

List of symbols and abbreviations

d	Initial particle diameter
d_{max}	Maximum particle diameter
e_0	Initial void ratio
n	Cyclic stress ratio
p'	Mean effective stress
q	Deviatoric stress
q_{cyc}	Cyclic deviatoric stress
q_f	Deviatoric stress at failure
AI	Angularity Index
AIMS	Aggregate Image Measurement System
BBI	Ballast breakage index
Bg	Marsal's index of particle breakage
CAPES	Coordenação de Aperfeiçoamento de Pessoal de Nível Superior
C_c	Coefficient of uniformity
CID	Isotropically consolidated drained
COPPE	Instituto Alberto Luiz Coimbra de Pós-Graduação e Pesquisa em Engenharia
CSL	Critical State Line
C_u	Coefficient of curvature
D	Specimen diameter
E	Elongation ratio
ESP	Effective Stress Path
F	Flatness ratio
FIOL	The West-East Integration Railway
F_f	Maximum fracture load
H	Specimen height

I	Particle's intermediate dimension
ISO	The International Organization for Standardization
L	Particle's longest dimension
M	Critical state friction coefficients
MT	Monotonic triaxial test
PSD	Particle size distribution
R^2	Coefficient of determination
S	Particle's shortest dimension
SP	Sphericity Index
TI	Texture Index
USA	The United States of America
USCS	Unified Soil Classification System
2D	Two dimensional
ε_a	Axial strain
ϕ'_{cv}	Friction angle at a constant volume (critical state)
σ_f	Characteristic particle tensile strength
σ_3	Confining pressure

References

- ABNT NBR 5564. (2021). *Via Férrea – Lastro Ferroviário – Requisitos e Métodos de Ensaio*. Associação Brasileira de Normas Técnicas, Rio de Janeiro (in Portuguese).
- ABNT NBR 6502. (1995). *Rochas e Solos - Terminologia*. Associação Brasileira de Normas Técnicas, Rio de Janeiro (in Portuguese).
- Al-Rousan, T.M. (2004). *Characterization of aggregate shape properties using a computer automated system* [PhD thesis]. College Station, Texas A&M University.
- American Railway Engineering Maintenance-of-way Association - AREMA. (2020). *Manual for railway engineering* (Vol. 1-4). Lanham: AREMA.
- Anderson, W.F., & Fair, P. (2008). Behavior of railroad ballast under monotonic e cyclic loading. *Journal of Geotechnical and Geoenvironmental Engineering*, 134(3), 316-327. [http://doi.org/10.1061/\(ASCE\)1090-0241\(2008\)134:3\(316\)](http://doi.org/10.1061/(ASCE)1090-0241(2008)134:3(316)).
- Aursudkij, B., McDowell, G., & Collop, A. (2009). Cyclic loading of railway ballast under triaxial conditions e in a railway test facility. *Granular Matter*, 11(6), 391. <http://doi.org/10.1007/s10035-009-0144-4>.
- Bishop, A.W., & Green, G.E. (1965). The influence of end restraint on the compression strength of a cohesionless soil. *Geotechnique*, 15(3), 243-266. <http://doi.org/10.1680/geot.1965.15.3.243>.
- Cescon, J.T.A.M. (2021). *Comportamento mecânico da mistura de lastro ferroviário com borracha de pneu* [Master's dissertation]. Instituto Militar de Engenharia.
- Cescon, J.T.A.M., Silva, B.-H.A., Marques, M.E.S., & Santos, R.P. (2021). Evaluation of the viability of recycling railroad ballast for reusing in railroads. *Research. Social Development*, 10(13), e277101321231. <http://doi.org/10.33448/rsd-v10i13.21231>.
- Chamling, P.K., Haldar, S., & Patra, S. (2020). Physico-chemical and mechanical characterization of steel slag

- as railway ballast. *Indian Geotechnical Journal*, 50(2), 267-275. <http://doi.org/10.1007/s40098-020-00421-7>.
- Delgado, B., Da Fonseca, A., Fortunato, E., & Motta, L. (2022). Particle morphology's influence on the rail ballast behaviour of a steel slag aggregate. *Environmental Geotechnics*, 9(6), 373-382. <http://doi.org/10.1680/jenge.18.00203>.
- Delgado, B.G., Fonseca, A.V., Fortunato, E., & Maia, P. (2019). Mechanical behavior of inert steel slag ballast for heavy haul rail track: laboratory evaluation. *Transportation Geotechnics*, 20, 100243. <http://doi.org/10.1016/j.trgeo.2019.100243>.
- Delgado, B.G., Fonseca, A.V., Fortunato, E., Paixão, A., & Alves, R. (2021). Geomechanical assessment of an inert steel slag aggregate as an alternative ballast material for heavy haul rail tracks. *Construction & Building Materials*, 279, 122438. <http://doi.org/10.1016/j.conbuildmat.2021.122438>.
- Esmacili, M., Yousefian, K., & Ghahroudi, P.A. (2020). An investigation of abrasion and wear characteristics of steel slag and granite ballasts. *Proceedings of the Institution of Civil Engineers - Construction Materials*, 173(1), 41-52. <http://doi.org/10.1680/jcoma.17.00044>.
- Esmacili, M., Yousefian, K., & Nouri, R. (2019). Vertical load distribution in ballasted railway tracks with steel slag and limestone ballasts. *The International Journal of Pavement Engineering*, 20(9), 1065-1072. <http://doi.org/10.1080/10298436.2017.1380808>.
- Festag, G., & Katzenbach, R. (2001). Material behaviour of dry sand under cyclic loading. In *Proceedings of the 15th International Conference on Soil Mechanics and Foundation Engineering* (pp. 87-90). Istanbul.
- Fletcher, T., Chandan, C., Masad, E., & Sivakumar, K. (2003). Aggregate imaging system for characterizing the shape of fine and coarse aggregates. *Transportation Research Record: Journal of the Transportation Research Board*, 1832(1), 67-77. <http://doi.org/10.3141/1832-09>.
- Gomes, M.B.B., Guimarães, A.C.R., Nascimento, F.A.C., & Santos, J.T.A. (2023a). Ballast with siderurgic aggregates: variation analysis of the shape parameters of particles submitted to triaxial tests through 3D scanner. *Soils and Rocks*, 46(3), e2023006122. <http://doi.org/10.28927/SR.2023.006122>.
- Gomes, M.B.B., Santos, J.T.A., Almeida, B.D., Serra, G.A., & Guimarães, A.C.R. (2023b). Análise paramétrica da espessura do lastro para deformações elastoplásticas no pavimento ferroviário. In *Anais do 25º Encontro Nacional de Conservação Rodoviária (ENACOR); 48ª Reunião Anual de Pavimentação (RAPv)* (pp. 193-202). Foz do Iguaçu. <http://doi.org/10.29327/1304307.48-18>.
- Greer, M., & Heitzman, M. (2017). *Evaluation of the AIMS2 and micro-deval to characterize aggregate friction properties. NCAT Report 17-02*. Auburn: NCAT.
- Guimarães, A.C.R., Costa, K.Á., Reis, M.M., Santana, C.S.A., & Castro, C.D. (2021). Study of controlled leaching process of steel slag in soxhlet extractor aiming employment in pavements. *Transportation Geotechnics*, 27, 100485. <http://doi.org/10.1016/j.trgeo.2020.100485>.
- Guo, Y., Markine, V., Song, J., & Jing, G. (2018). Ballast degradation: effect of particle size and shape using Los Angeles Abrasion test and image analysis. *Construction & Building Materials*, 169, 414-424. <http://doi.org/10.1016/j.conbuildmat.2018.02.170>.
- Guo, Y., Markine, V., Zhang, X., Qiang, W., & Jing, G. (2019). Image analysis for morphology, rheology and degradation study of railway ballast: A review. *Transportation Geotechnics*, 18, 173-211. <http://doi.org/10.1016/j.trgeo.2018.12.001>.
- Ibiapina, D.S., Castelo Branco, V.T.F., Diógenes, L.M., Motta, L.M.G., & de Freitas, S.M. (2018). Proposição de um sistema de classificação das propriedades de forma de agregados caracterizados com o uso do processamento digital de imagens a partir de materiais oriundos do Brasil. *Transportes*, 26(4), 116-128. <http://doi.org/10.14295/transportes.v26i4.1510>.
- Indraratna, B., & Ngo, T. (2018). *Ballast railroad design: smart-uow approach*. CRC Press. <http://doi.org/10.1201/9780429504242>
- Indraratna, B., & Salim, W. (2003). Deformation and degradation mechanics of recycled ballast stabilized with geosynthetics. *Soil and Foundation*, 43(4), 35-46. http://doi.org/10.3208/sandf.43.4_35.
- Indraratna, B., Ionescu, D., & Christie, H.D. (1998). Shear behaviour of railway ballast based on large-scale triaxial test. *Journal of Geotechnical and Geoenvironmental Engineering*, 124(5), 439-449. [http://doi.org/10.1061/\(ASCE\)1090-0241\(1998\)124:5\(439\)](http://doi.org/10.1061/(ASCE)1090-0241(1998)124:5(439)).
- Indraratna, B., Lackenby, J., & Christie, D. (2005). Effect of confining pressure on the degradation of ballast under cyclic loading. *Geotechnique*, 55(4), 325-328. <http://doi.org/10.1680/geot.2005.55.4.325>.
- Indraratna, B., Qi, Y., Tawk, M.H.A., Rujikiatkamjorn, C., & Navaratnarajah, S.K. (2022). Advances in ground improvement using waste materials for transportation infrastructure. *Proceedings of the Institution of Civil Engineers: Ground Improvement*, 175(1), 3-22. <http://doi.org/10.1680/jgrim.20.00007>.
- Indraratna, B., Shahin, M.A., & Salim, W. (2007). Stabilisation of granular media and formation soil using geosynthetics with special reference to railway engineering. *Ground Improvement*, 11(1), 27-43. <http://doi.org/10.1680/jgrim.2007.11.1.27>.
- Indraratna, B., Tennakoon, N., Nimbalkar, S., & Rujikiatkamjorn, C. (2013a). Behaviour of clay-fouled ballast under drained triaxial testing. *Geotechnique*, 63(5), 410-419. <http://doi.org/10.1680/geot.11.P.086>.
- Indraratna, B., Hussaini, S.K.K., & Vinod, J.S. (2013b). The lateral displacement response of geogrid-reinforced ballast under cyclic loading. *Geotextiles and Geomembranes*, 39, 20-29. <http://doi.org/10.1016/j.geotxmem.2013.07.007>.
- Indraratna, B., Wijewardena, L.S.S., & Balasubramaniam, A.S. (1993). Large-scale triaxial testing of greywacke rockfill. *Geotechnique*, 43(1), 37-51. <http://doi.org/10.1680/geot.1993.43.1.37>.

- Ionescu, D. (2004). *Evaluation of the engineering behaviour of railway ballast* [PhD thesis]. University of Wollongong. ISO 17892-9. (2018). *Geotechnical investigation and testing — Laboratory testing of soil — Part 9: Consolidated triaxial compression tests on water saturated soils*. International Organisation for Standardisation, Geneva.
- Jaeger, J.C. (1967). Failure of rocks under tensile conditions. *International Journal of Rock Mechanics and Mining Sciences & Geomechanics Abstracts*, 4(2), 219-227. [http://doi.org/10.1016/0148-9062\(67\)90046-0](http://doi.org/10.1016/0148-9062(67)90046-0).
- Jing, G., Wang, J., Wang, H., & Siahkouhi, M. (2020). Numerical investigation of the behavior of stone ballast mixed by steel slag in ballasted railway track. *Construction & Building Materials*, 262, 120015. <http://doi.org/10.1016/j.conbuildmat.2020.120015>.
- Klincevicius, M.G.Y. (2011). *Estudo de propriedades, de tensões e do comportamento mecânico de lastros ferroviários* [Dissertação de mestrado]. Universidade de São Paulo.
- Lade, P.V., Yamamuro, J.A., & Bopp, P.A. (1996). Significance of particle crushing in granular materials. *Journal of Geotechnical Engineering*, 122(4), 309-316. [http://doi.org/10.1061/\(ASCE\)0733-9410\(1996\)122:4\(309\)](http://doi.org/10.1061/(ASCE)0733-9410(1996)122:4(309)).
- Lee, D.M. (1992). *The angles of friction of granular fills* [Ph.D. dissertation]. University of Cambridge.
- Marsal, R.J. (1965). Soil properties-shear strength and consolidation. In *Proceedings of the 6th International Conference on Soil Mechanics and Foundation Engineering* (Vol. 3, pp. 310-316). Montreal.
- Masad, E. (2003). *The Development of a Computer Controlled Image Analysis System for Measuring Aggregate Shape Properties: Final Report for Highway-IDEA Project 77*. Transportation Research Board
- McDowell, G.R., & Bolton, M.D. (1998). On the micromechanics of crushable aggregates. *Geotechnique*, 48(5), 667-679. <http://doi.org/10.1680/geot.1998.48.5.667>.
- Mvelase, G.M., Anochie-Boateng, J.K., & Grabe, P.J. (2012). Application of laser based technology to quantify shape properties of railway ballast. *Proceedings of the 31st Southern African Transport Conference (SATC 2012)* (Vol. 2, pp. 243-254). Pretoria, South Africa.
- Nakata, Y., Kato, Y., & Murata, H. (2001). Properties of compression and single particle crushing for crushable soil. *Proceedings of 15th International Conference on Soil Mechanics and Foundation Engineering* (Vol. 1, pp. 215-218). Istanbul.
- Paixão, A., Fortunato, E., & Calçada, R. (2016). A numerical study on the influence of backfill settlements in the train/track interaction at transition zones to railway bridges. *Proceedings of the Institution of Mechanical Engineers. Part F, Journal of Rail and Rapid Transit*, 230(3), 866-878. <http://doi.org/10.1177/0954409715573289>.
- Raymond, G.P., & Diyaljee, V.A. (1994). Railroad ballast sizing and grading. *Journal of the Geotechnical Engineering Division*, 105(5), 676-681. <http://doi.org/10.1061/AJGEB6.0000803>.
- Rede Ferroviária Nacional – REFER. (2015). *RF.IT.VIA.015. Especificações técnicas para fornecimento de balastro novo*. REFER.
- Rosa, A.F. (2019). *Efeito da granulometria e da litologia no comportamento de lastros ferroviários em laboratório e por análise computacional* [Master's dissertation]. Universidade Federal do Rio de Janeiro.
- Rosa, A.F., Aragão, F.T.S., & Motta, L.M.G. (2021). Effects of particle size distribution and lithology on the resistance to breakage of ballast materials. *Construction & Building Materials*, 267, 121015. <http://doi.org/10.1016/j.conbuildmat.2020.121015>.
- Saint-Cyr, B., Voivret, C., Delenne, J.-Y., Radjai, F., Sornay, P., Nakagawa, M., & Luding, S. (2009). Effect of shape nonconvexity on the shear strength of granular media. *AIP Conference Proceedings*, 1145(1), 389-392. <http://doi.org/10.1063/1.3179941>.
- Santos, J.T.A., Gomes, M.B.B., Guimarães, A.C.R., Nascimento, F.A.C., Santos, L.H., & Junior, C.J.A. (2022). Caracterização geotécnica e análise do comportamento resiliente de solos tropicais para aplicação em sublastro ferroviário. In *Anais do 24º Encontro Nacional de Conservação Rodoviária (ENACOR); 47ª Reunião Anual de Pavimentação (RAPv)* (pp. 760-771). Bento Gonçalves: ABPv.
- Selig, E.T., & Waters, J.M. (1994). Track geotechnology and substructure management. Thomas Telford. <http://doi.org/10.1680/tgasm.20139>.
- Silva, F.H.P. (2018). *Estudo do comportamento de um lastro ferroviário sob carga repetida em modelo físico de verdadeira grandeza* [Master's dissertation]. Universidade Federal do Rio de Janeiro.
- Skoglund, K., Hoseth, S., & Værnes, E. (2000). Development of a large triaxial cell apparatus with variable deviatoric and confining stresses. *Unbound Aggreg Road Constr UNBAR*, 4, 145-152.
- Suiker, A.S., Selig, E.T., & Frenkel, R. (2005). Static e cyclic triaxial testing of ballast e subballast. *Journal of Geotechnical and Geoenvironmental Engineering*, 131(6), 771-782. [http://doi.org/10.1061/\(ASCE\)1090-0241\(2005\)131:6\(771\)](http://doi.org/10.1061/(ASCE)1090-0241(2005)131:6(771)).
- Suiker, A.S.J. (2002). *The mechanical behaviour of ballasted railway tracks* [PhD thesis]. Delft University of Technology.
- Tafesse, S., Fernlund, J.M.R., & Bergholm, F. (2012). Digital sieving-Matlab based 3-D image analysis. *Engineering Geology*, 137-138, 74-84. <http://doi.org/10.1016/j.enggeo.2012.04.001>.
- Tutumluer, E., Mishra, D., & Butt, A.A. (2009). *Characterization of Illinois aggregates for subgrade replacement and subbase* (Illinois Center for Transportation Series, No. 09-060). Illinois Center for Transportation.
- Werkmeister, S., Dawson, A.R., & Wellner, F. (2001). Permanent deformation behavior of granular materials and the shakedown concept. *Transportation Research Record: Journal of the Transportation Research Board*, 1757(1), 75-81. <http://doi.org/10.3141/1757-09>.
- Zingg, T. (1935). Bietrahe zur Schotteranalyse. *Schweiz Mineral Petrography*, 15, 139-140. [in German].